Journal of Engineering and Applied Sciences 12 (Special Issue 9): 8547-8559, 2017
ISSN: 1816-949X

Investigating the Effect of Underwater Explosion on Sandwich Structures

[1]Hassan Bagheri, [2]Aman Allah Shabankareh and [3]Mohammad Safi
[1]Department of Technical, Bushehr Port and Maritime (BPMO), Telghani Ave, Bushehr, Iran
[2]Yasouj Branch, Islamic Azad University, Yasouj, Iran
[3]Department of Civil and Environmental Engineering, Shahid Beheshti University, Tehran, Iran

Abstract: Underwater explosion is one of the most destructive phenomena in offshore and coastal structures. Therefore, any country connected to free waters requires foresight regarding retrofit of offshore ship and structures. Although, designing a structure based on explosive loads is not affordable, investigating the waves caused by explosion and their destructive effects could take into account some considerations in locating and constructing of these structures, so that, the minimum destruction would occur. Given the necessity of this issue and what mentioned above, the results of evaluating dynamic behavior of honeycomb sandwich structures under underwater explosion can be examined using finite element method and simulating the explosion environment. In this regard, this study has modeled and monitored 5 samples of honeycomb structures with different cores by simulating them to evaluate the dynamic behavior in underwater explosion condition using explicit dynamic. The results indicated that ductility against underwater explosive load depends on the structure core for honeycomb sandwich structures and this is frequently shown in figures, deformations and contours. Also, the results indicated that a honeycomb structure with diagonal and discrete core has the minimum and maximum deflection equal to 6.2 and 19 cm, respectively. Other samples including square, circular and hexagonal core has 41, 20 and 23% less deformation than the discrete sample. In other words, diagonal sandwich structures are more resistant against the waves caused by underwater explosion and show a more optimal behavior.

Key words: Underwater explosion, sandwich structures, finite element method, gas bubble, explosive load, samples

INTRODUCTION

Generally, since, marine industries, namely cruise and cargo ships, military vessels, offshore platforms, ports and harbors have always been built with high economic costs and put into operation, their capacity against perilous and massive loads must be controlled, depending on their importance by applying a specific approach during analysis and scheme and even construction and maintenance. Nowadays, advances in studies and research indicate that various parameters determine the behavior and function of the structures. This has followed its rising trend during investigating the interaction between structure and soil or structure and water and incorporating their effects in design and analysis. However, for cases in which besides service loads it is possible that the structure tolerates massive unexpected loads such as explosion waves, investigating the effect of this kind of destructive loads on structure behavior might be important. Explosion can occur for economic capital of any country due to the threat of terrorist attacks, war or even completely randomly in some cases. Underwater explosion is considered a big treat in offshore structures as they are not designed to serve the pressure caused by explosion waves while the power of wave transmission in water is much more than that in air. Another important challenge that the researchers in this area have always faced is proper experience and perception of what is applied to the structure under underwater explosion. In other words, several years of planning is required to make laboratory and even real, simulations in certain locations by spending significant economic costs and obtained the desired results (Aruk, 2008). The necessity of importance of sandwich structures such as honeycomb ones is because this kind of structures are now servicing in extensive areas of industry and technology. Storage tanks, nuclear facilities, submarine hull and foundation of tall buildings are a few examples of common applications of these structures. Precise prediction onhow this kind of structures gets damaged by explosions is the main concern of Structural and Mechanical Engineering. Performing experiments to determine how these structures

Corresponding Author: Hassan Bagheri, Department of Technical, Bushehr Port and Maritime (BPMO), Telghani Ave, Bushehr, Iran

respond to the waves caused by explosion or whether they get damaged is very expensive and time consuming. Environmental protection is another constraint of experimental tests. On the contrary, development and creation of analytical solutions for dynamic response of the structure to the explosion phenomenon is difficult due to complexity of the structural model and structure-fluid (air) interaction. Therefore, the theoretical studies in this context on specific structural models under impact wave load, bubble dynamics and fluid-structure interaction seem necessary. On the other hand, honeycomb structures are among the structures introduced into important industries and their application is increasingly growing. According to what was mentioned above, evaluating the resistance of honeycomb structures against the loads caused by explosion is an important factor in determining the overall safety of the structure, so that, investigating the effect of explosion on offshore structures, construction of which usually imposes significant costs for the countries, seems necessary.

Underwater explosion has remained a treat for human facilities and a challenge for the researchers even after a century. The World War II might be the beginning of emergence of this issue as many naval vessels faced it from mines and submarines, following which extensive studies were carried out in the area of underwater explosion (Aruk, 2008). Many of these studies were performed on the effect of underwater explosion components on submarines and ship hulls. Meanwhile, the majority of the studies were performed focusing on the primary pressure wave caused by the explosion while the extent of studies performed on secondary pulse of the pressure caused by air bubble is significantly less than that of the first phase (Krueger, 2006). In 1989, US Defense Ministry addressed the features and characteristics of the shock tests caused by underwater explosion on ship hull in a technical report and presented some results regarding acceleration, velocity and displacement of the system in different positions and also expressed the stresses and elastic deformations imposed on the structure during experiencing this process (Anonymous, 1989). The results obtained by this report and the method of performing this test are used in many studies (Aruk, 2008). Zhang and Geers (1993) carefully analyzed and formulated a shell structure submerged in a sphere environment under the influence of plane waves. Sprague and Geers (1999) extended the research conducted by Zhang and Geers (1993) and explained the exponential function of expansion of spherical waves caused by underwater explosion (Sprague and Geers, 1999). Shane *et al*. (2007) evaluated an integrated beam and a beam with sandwich perforated core in their research using finite element method and investigated their sensitivity in terms of the degree of compaction and type of beam core against the waves caused by under water explosion (Shane *et al*., 2007). The same year, Klenow and Brown (2007) examined water-structure interaction under explosion in water depth in their study. They also discussed the conventional assumptions of the equations governing the acoustic environment and confirmed their limitations (Klenow and Brown, 2007). Following that, Hung *et al*. (2009) evaluated the dynamic response of cylindrical plated submerged under the waves caused by explosion in their research, using linear and non-linear analyses. To do so, they placed a small charge at a distance of 35-210 cm and observed the plastic behavior at a distance >50 cm from the samples under study (Hung *et al*., 2009). Recently, investigated the long-term vibration caused by underwater explosion in their study. To do so, they invented a new method to perform their experiments. This study has discussed and analyzed single and successive vibrations caused by underwater explosion in different time steps (Sheng *et al*., 2012).

MATERIALS AND METHODS

Theory of underwater explosion: Generally, a significant amount of gas and energy will be generated by underwater explosion which is the result of a shock wave (Cole, 1948). In this regard, the first step of completion of this reaction is explosion of explosive materials such as TNT and HBX-1 in water depth, following which the shock wave mentioned above will propagate in the explosive material as pressure waves. Along this reaction, other reactions will occur as well which will lead to generation and increment of pressure waves, so that, the explosive materials with high pressure and temperature transfer from solid state to gas state during this process (approximately 3000°C temperature and 500 MPa pressure). The rate of this process is initially in the order of nanoseconds and greater than the sound velocity. However, since, this reaction occurs under the water its rate exponentially decreases from 25,000-5,000 ft/sec (sound velocity in water) (Cole, 1948; Aruk, 2008; Krueger, 2006). The main difference between explosion in water and air is the dynamics of gas core resulted from explosion of the explosive material (bubble) and since, water is able to control these gasses a bubble will be formed (Fig. 1) (Mazaheri and Taheri, 2003). There are many relations available to determine shock wave, the most important examples of which are Kirkwood and Beth or Penny relations to name a few (Cole, 1948). The shock wave is created in <7-10 sec, then it is adds to the water

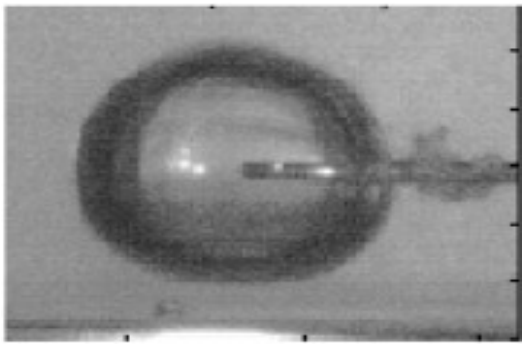

Fig. 1: Formation of bubble by explosion (Zhang *et al*., 2009)

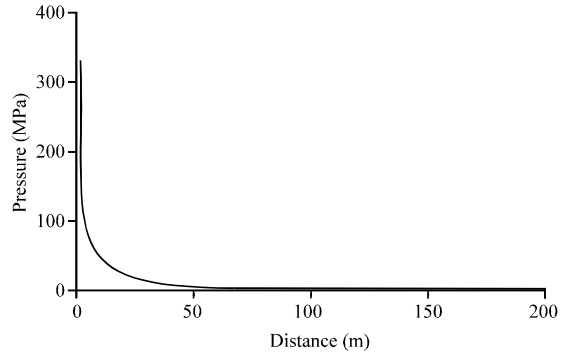

Fig. 2: Decrease in maximum shock wave pressureby increasing the distance from target point (136 kg-TNT)

hydrostatic pressure and then gradually decreases. The history of this pressure in explosion Point (Pt) (Eq. 1) is calculated by a maximum Pressure (Pm) at its instant moment (Eq. 2). This Pressure (Pm) is a function of the distance and charge used in the explosive material. Figure 2 shows the decrease in maximum pressure in 1-200 m from the target point for 137 kg TNT. In Eq. 1, θ is a time decrement and "t" would be expressed in the interval of 0-θ. Equation 3 is obtained based on charge and distance. It is obvious that increasing distance results in exponential increase in θ, along with decrease in Pt. it has to be noted that in all three equations, W is the weight of the explosive material (TNT) in kg and R is its distance from the target (Cole, 1948; Rajendran and Narasimhan, 2006):

$$P_t = P_m.e^{(-t/\theta)} \quad (1)$$

$$P_m = 52.16\left(\frac{W^{1/3}}{R}\right)^{1.13} \quad (2)$$

$$\theta = 96.5(W^{1/3})\left(\frac{W^{1/3}}{R}\right)^{-0.22} \quad (3)$$

Equation 1 is used to determine the pressure resulted from the explosion of any amount of explosive materials (from small amounts to huge amounts transmitted from nuclear weapons) at any depth, except at the vicinity of the charge (almost 10 times its radius) in which the maximum shock wave is greater than what is predicted by the formula (Rajendran and Narasimhan, 2006). Moreover, the impact of the imposed force (in Nsec/m^2) and the total energy of the system (J/m^2) are estimated from Eq. 4 and 5, respectively (Rajendran and Narasimhan, 2006; Gupta *et al*., 2010):

$$I = \int_0^\infty P_t dt = 5760(W^{1/3})\left(\frac{W^{1/3}}{R}\right)^{0.891} \quad (4)$$

$$E = \frac{1}{\rho c}\int_0^\infty P_t^2 dt = 98000(W^{1/3})\left(\frac{W^{1/3}}{R}\right)^{2.1} \quad (5)$$

Parameters ρ and c in Eq. 5 are water density (kg/m^3) and sound velocity (m/sec). The sudden release of energy caused by explosion of a strong explosive material leads to formation of a bubble with high pressure and very high temperature, following which shock wave will be created in the water. Studies has shown that 12 gas bubble pulses will be created by using an explosive material, the first pulse of which will have a pressure almost 10-15% of the maximum instant pressure (Eq. 2). Along with formation of these pulses, the bubbles will be transferred to the water surface due to pull of gravity (Gupta *et al*., 2010).

This transfer occurs in a certain time interval along with the bubble fluctuations and the pressure wave in positive and negative phases and finally returns to its initial hydrostatic pressure after the collapse of the environment bubble (Fig. 3). Meanwhile, two critical parameter, i.e., the maximum bubble radius occurring at the first pulse of formation and the pulse periods are of great importance. These two parameters are expressed by Eq. 6 and 7:

$$R_{max} = 3.3\left(\frac{W}{Z}\right)^{1/3} \quad (6)$$

$$T = 2.08\left(\frac{W^{1/3}}{Z^{5/6}}\right) \quad (7)$$

Where:

W = The Weight of the explosive material (TNT)

Z = Total hydrostatic pressure at charge location which is equal to:

$$Z = D+10 \quad (8)$$

where, D is the depth of the explosive material from water surface. Figure 4 shows the changes in bubble radius which exponentially decreases up to 15 m depth from water surface, assuming a charge of 136 kg TNT (Rajendran and Narasimhan, 2006). Assuming little movement, compressible fluid and adiabatic process, the equilibrium equation for fluid particles is related to the energy loss of the momentum-dependent velocity by the Eq. 9:

$$\frac{\partial P}{\partial x} + \gamma \dot{U}^f + \rho_f \ddot{U}^f = 0 \quad (9)$$

Where:

P = The excess fluid pressure (the pressure in addition to static pressure)
x = The fluid particle location
$\dot{U}^f$ = The fluid particle velocity
$\ddot{U}^f$ = Fluid particle acceleration
ρ_f = The fluid density
γ = Volumetric drag (force/unit volume-velocity)
θ_i = An independent variable (e.g., temperature, humidity or salinity which might depend on density and volumetric drag)

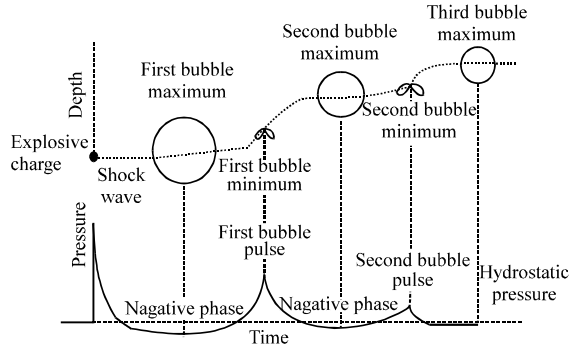

Fig. 3: Gas bubble fluctuations and their corresponding pressure in underwater explosion (Krueger, 2006)

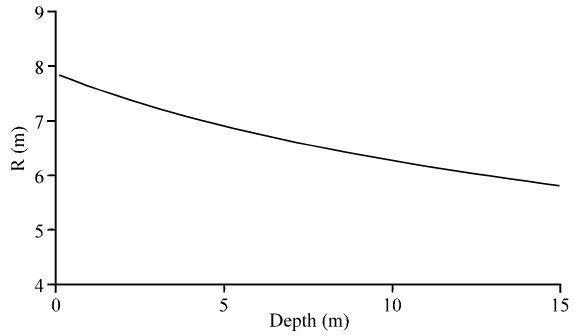

Fig. 4: Changes in gas bubble radius at depth

The terms of D'Alembert equation were neglected, assuming continuous fluid flow and without considering the terms of convection acceleration. This assumption is fairly accurate for continuous fluid flow with the velocity up to Mach number 0.1. Assuming non-viscous, linear and compressible fluid, Eq. 10 will be obtained:

$$P = K_f(x, \theta_i)\frac{\partial}{\partial x}U^f \quad (10)$$

where, K_f is the fluid bulk modulus. Other parameters were described in Eq. 9. For a fluid without possibility of cavitation, the total fluid pressure (dynamic and static pressures) cannot be less than cavitation pressure. When there is possibility of cavitation, fluid pressure decreases to less than cavitation pressure.

RESULTS AND DISCUSSION

Finite element simulation and experimental validation: A 25×30 cm^2 plate is modelled in this study for numerical study of its behavior under the explosion of 10, 20 and 40 g TNT at the depth of 2 m from water surface which was previously experimentally analyzed by Ramajeyathilagam and Vendhan (2004) using ABAQUS Software and the validity of the results are evaluated. The plate thickness is 2 mm. Figure 5 shows a picture of the plate and its positioning under the water. In order to apply the acoustic conditions prevailing, water is modelled as a spherical model. The initial water depth is assumed to be 2 m for all models and the sound velocity in water is taken as 1500 m/sec. The physical properties of underwater explosion charge are given in Table 1, the charge material properties are given in Table 2 and the properties of the bubbles resulted from this explosion are given in Table 3. All these values are fed to the software.

Fig. 5: Experimental test sample (Ramajeyathilagam and Vendhan, 2004)

Table 1: Charge physical properties

Variables	Values
Gas specific heat ratio	1.27
Gravitational acceleration (m/sec^2)	9.81
Atmospheric Pressure (Pa)	98000
Flow drag coefficient	2
Flow drag exponent	2

Table 2: Charge material properties

Contants	Values
Constant K	52100000
Constant k	9.00E-05
Constant A	0.18
Constant B	0.185
Constant K_c	8.4E+08
Charge density (kg/m^3)	1500
Charge mass (kg)	1

Table 3: Produced bubbles properties

Parameters	Values
Time duration (sec)	1
Max number steps	4.00E+04
Relative control	1.00E-19
Absolute control	1.00E-19
Control exponent	0.2

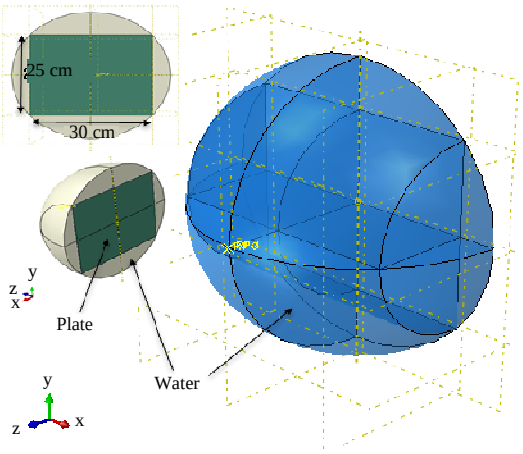

Fig. 6: Schematic of plate status and charge position

The location of explosion and standoff point in the software will be referred to as reference point 1 and 2, respectively. The software analyzes the spacing between source point and standoff point with an appropriate approximation and then precisely analyzes the distance between standoff point and the target. Similar to the experimental model, the charge used is positioned 15 cm from the plate (standoff distance) in this numerical simulation (Fig. 6). Figure 7 shows the status of plate and its surrounding spherical water simulated as the spherical waves of explosion (Table 4).

The plate mentioned above was meshed and modelled in ABAQUA Software along with its own fluid (Fig. 7). Figure 8 shows the meshed components in

Table 4: Charge physical properties

Parameters	Values
Gas specific heat ratio	1.27
Gravitational acceleration (m/sec^2)	9.81
Atmospheric pressure (Pa)	98000
Flow drag coefficient	2
Flow drag exponent	2

Table 5: Properties of the simulated material

Steel/Variables	Values
Steel	
Young modulus	210000 (MPa)
Poisson's ratio	0.3
Density	7800 (kg/m^3)
Yield stress	300 (MPa)
Water	
Density	1050 (kg/m^3)
Bulk modulus	2068 (MPa)

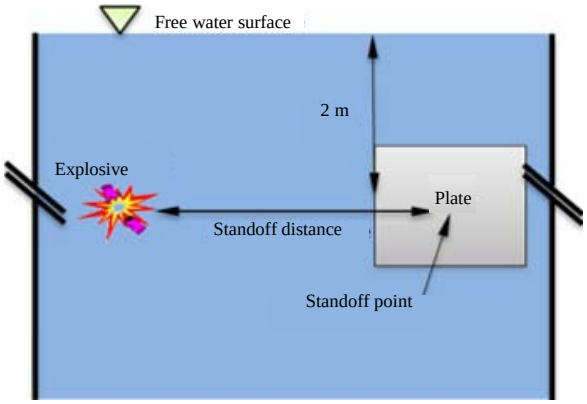

Fig. 7: Status of the plate and its surrounding water simulated

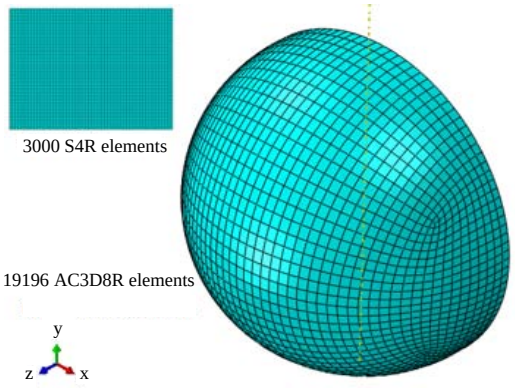

Fig. 8: Plate and fluid mesh

this modelling with the explanations of software element family. The consumption material introduced to the software is steel with density of 7850 kg/m^3 and Poisson's ratio of 0.3 (Table 5).

Figure 7 shows acoustic pressure distribution in 4 different time steps during the analysis

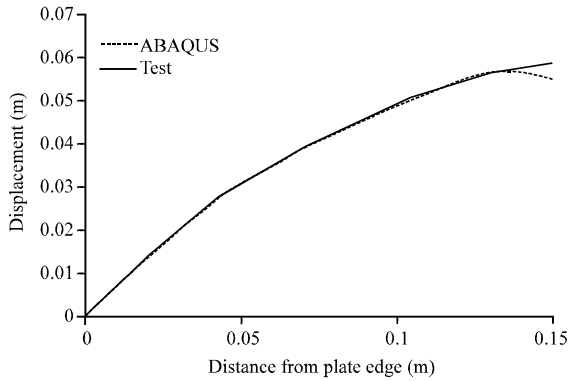

Fig. 9: Deformation in the middle of the page under explosion of 20 g TNT

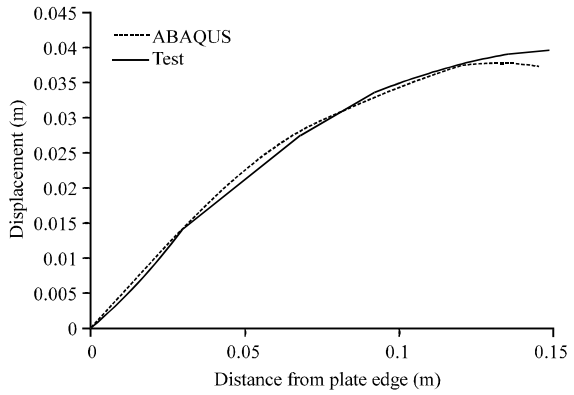

Fig. 10: Deformation in the middle of the plate under explosion of 10 g TNT

process. Figure 1 and 4 are selected from the initial and final stages of pressure distribution, respectively and Fig. 2 and 3 are selected from the middle stages of pressure distribution.

Moreover, Fig. 7 shows the deformations caused by explosion by acoustic pressures in 2 and 3D spaces as well as two horizontal and vertical layers from the meshes among the plate to monitor von Mises stresses. The maximum amount of this stress in the middle node is more than 1.6e+8 N/m^2. Selecting a hemisphere to simulate acoustic environment as well as symmetry of rectangular plate along the path of propagation of the waves caused by underwater explosion has led to equal changes in stress in the two layers (Fig. 9). In addition, to control the structure response, the behavior of the middle node in the plate was controlled. Figure 10 shows the displacement of this node during analysis (0.003). The maximum displacement of this node under explosion of 1 kg TNT at 1 m distance is almost 23 mm.

After analyzing the structure by software processor, the displacement of middle nodes were extracted from

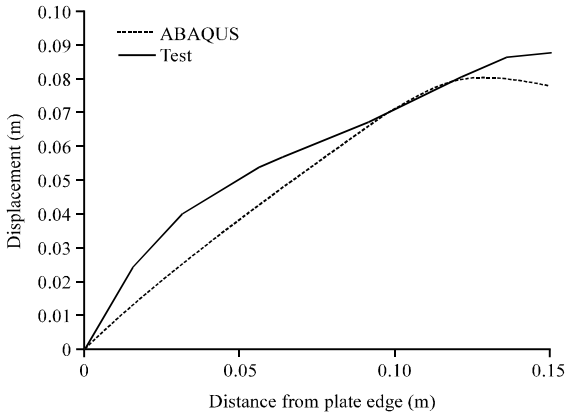

Fig. 11: Deformation in the middle of the page under explosion of 40 g TNT

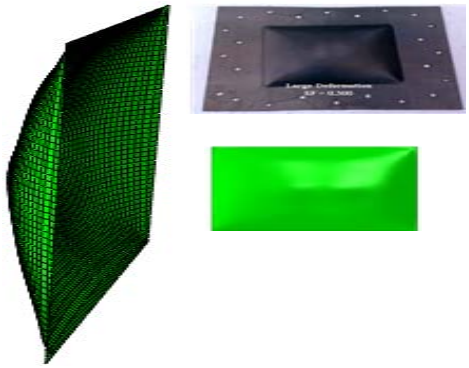

Fig. 12: Experimental and numerical deformation of the structure

Ramajeyathilagam and Vendhan (2004) and were compared with software results. The chargees applied were considered to analyze 10, 20 and 40 kg TNT. Figure 9-11 show the deformation in the middle of structure plant under 10, 20 and 40 kg charge applied, respectively. As it is clear from the figures mentioned before, the results obtained by structure analysis and experimental test were consistent and the accuracy of ABAQUS Software in this analytical method, considering and simulating the surrounding water is significant.

Figure 12 schematically shows deformation of the structure under explosion of 10 g TNT in the laboratory with numerical example. This deformation also has a reasonable accuracy. According to middle plate deformations and Fig. 9-11, the plate stress can be examined in different charge states. It is clear from Fig. 13-15 that the Mises stresses have reached yield stress (300 MPa) when the charge is 10, 20 and 40 g TNT and the structure is at plastic state.

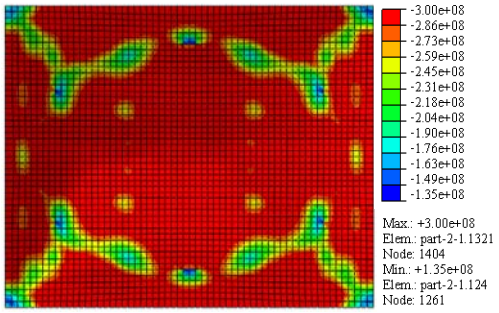

Fig. 13: Mises stress contours in the plate under explosion of 10 g TNT

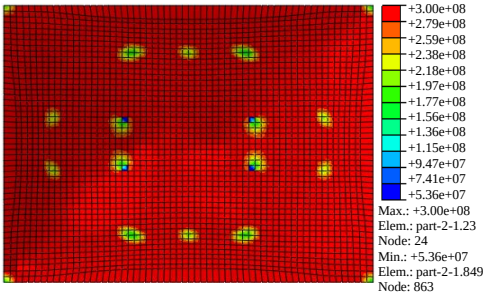

Fig. 14: Mises stress contours in the plate under explosion of 20 g TNT

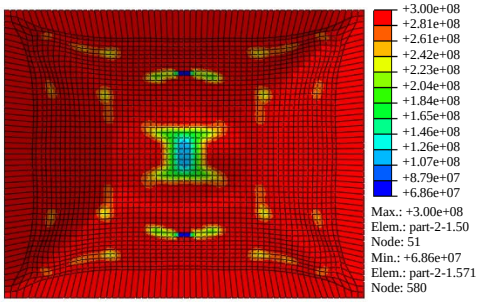

Fig. 15: Mises stress contours in the plate under explosion of 40 g TNT

Parametric study of sandwich structures: Since, the purpose of this study is investigating the effect of underwater explosion on sandwich and honeycomb structures, models have been selected for parametric study. Over 500 types of sandwich structures have been introduced by the researchers and implemented in the industry so far. This applied study discusses some of the most functional and pervasive examples of these models in underwater structures (Fig. 1-5). These models include square honeycomb structure, diagonal honeycomb structure, circular honeycomb structure, hexagonal honeycomb structure and discrete honeycomb

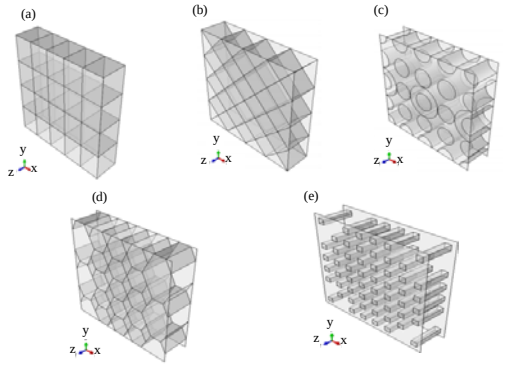

Fig. 16: Introduction to the honeycomb structures used in this study; a) Square honeycomb structure; b) diagonal honeycomb structure; c) Circular honeycomb structure; d) Hexagonal honeycomb structure and e) Discrete honeycomb structure

Table 6: The amount of sheet used in core layer of numerical models

Core type	Model name	Core area (m^2)
Diagonal	Dia.	11.5
Honeycomb	Hex.	11.2
Simple-square	Sq.	11.0
Discrete	Dis.	11.2
Circular	Cir.	11.1

Table 7: Charge properties and distance of the explosive material

	Distance (m)	
Target to standoff point	Standoff point to source point	Amount of charge (kg TNT)
1	2.1	40
1	4.7	40
1	9.3	40

structure, all shown in Fig. 16. In all models, the middle layer sheets (core) are used almost = 11.3 m^2. Table 6 shows the amount of sheet used in the core of all models. Thickness of all sheets including the surfaces and the core is considered to be 7 mm which is increased to 12 mm in the analysis in order to evaluate the effect of core thickness.

The element used for the upper, lower and core layers of all sandwich structures mentioned above is S4R (shell, 4-node, reduced integral method) while the element used for water simulation is AC3D8R (acoustic, continuous, 3D, 8-node, reduced integral method). The number of square, diagonal, circular, hexagonal and discrete elements is 7600, 7960, 8449, 7353 and 8063, respectively. The number of elements is the water model is also 13208. The properties of explosive charge source distance to the upper surface of sandwich structures, charge positioning and amount of the charge are shown in Table 7. According to Table 7, two different charges are applied at two different distances to analyze structure response under underwater explosion.

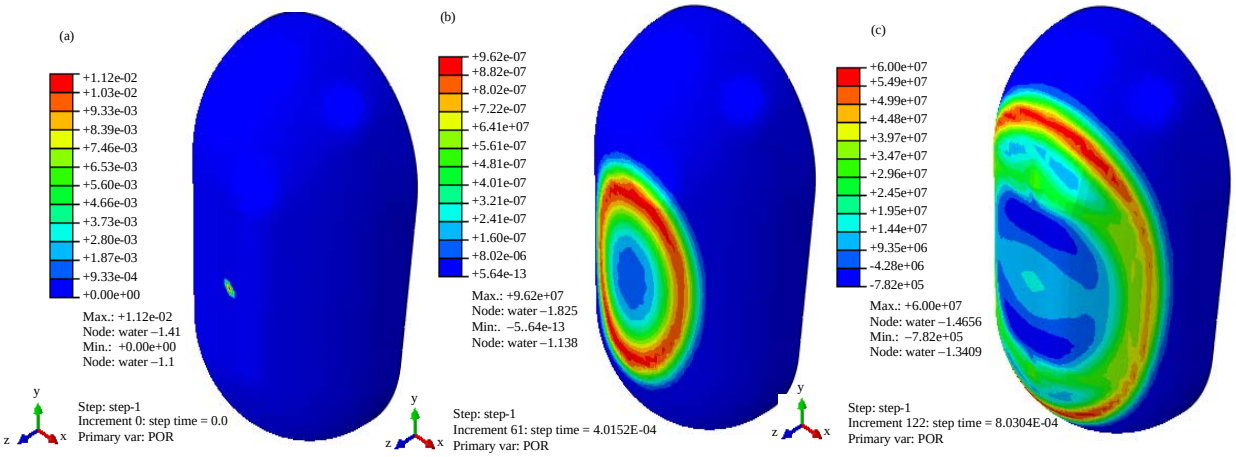

Fig. 17: Pressure changes in acoustic environment from 0 to 0.0008 sec: a) Acoustic environments pressure 0 sec; b) Acoustic environments pressure 0.0004 sec and c) Acoustic environments pressure 0.0008 sec

Investigating the changes in water pressure during explosion: One of the most important results of this study is the extent of pressure changes in acoustic environment. These changes are determined based on the code specified in the software at 21 stages of solution by ABAQUS Software solver. The maximum pressure at the beginning of the explosion of 40 g TNT occurred as the explosive charge at 0.0004 sec (Fig. 17) was 96 MPa which gradually decreased by 70% up to the end of analysis with a significant jump. It is worth noting that the maximum acoustic pressure occurred in a direct line between the charge and structure.

Analyzing the behavior of structures under explosion of 40 kg TNT: In order to analyze the structure, the initial charge was considered to be 40 kg TNT, positioned at 3 m distance from the samples. The maximum stress exerted on square honeycomb structure from 0 to 0.0008 sec was 138 MPa. This maximum stress in the middle layer (core of the structure) occurred in 0.0068 sec and pressed down the surface plate component by 13.82 cm. The final displacement of the structure after 0.0008 sec in shown in Fig. 18. Figure 19 also shows the history of the surface plate deformation, based on which it can be inferred that the changes became non-linear after about 0.0015 sec and the structure approached yield point. Another point to be noted is ultimate strain changes in the structure. The in-plane strain was equal to 0.068 which was greater than the strain in the peripheral areas facing the upper surface while the lower surface experienced a maximum strain of 0.008 (Fig. 20 and 21).

In this study, the behavior of circular sandwich structure is compared with that of square one, under the same charge of 40 kg TNT. Stress contours at 0.0008, 0.0016 and 0.0028 sec after explosion was investigated.

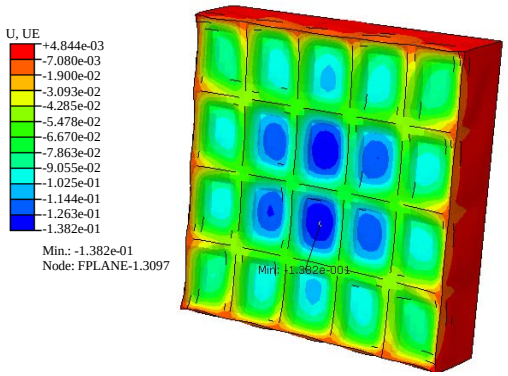

Fig. 18: Deformation contour in square honeycomb surface under explosion of 40 kg TNT

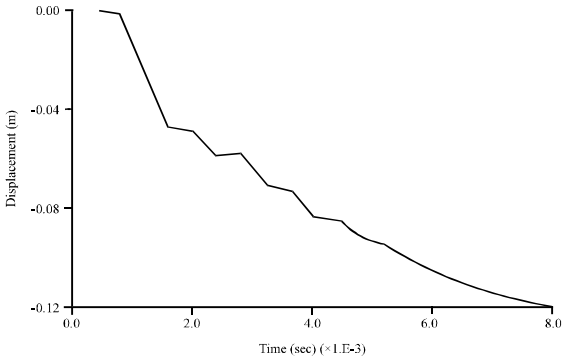

Fig. 19: Time history of deflection of square honeycomb surface

The maximum Mises stress at 0.0028 sec was 178 MPa which was decreased by 23% compared to the square sample. The structure deformation contour is shown in

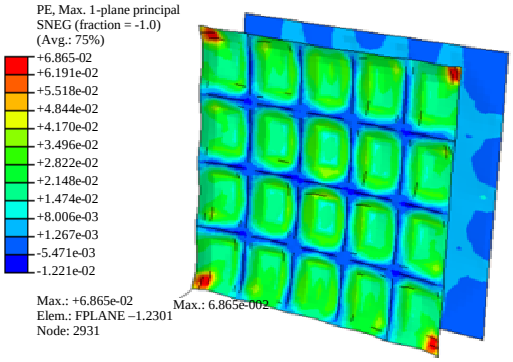

Fig. 20: Strain contours in square sample upper surface under explosion of 40 kg TNT

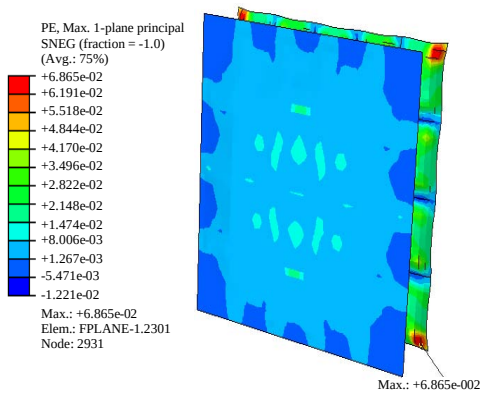

Fig. 21: Strain contours in square sample lower surface under explosion of 40 kg TNT

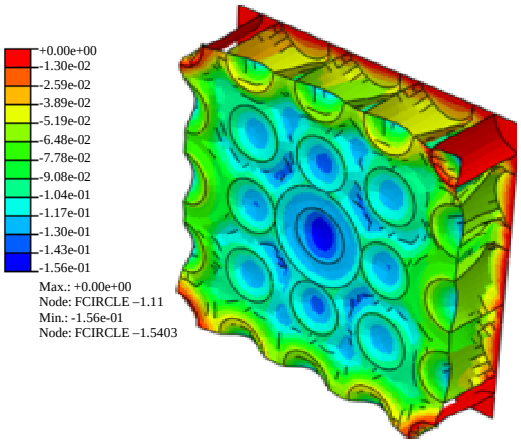

Fig. 22: Deformation contour in square honeycomb surface under explosion of 40 kg TNT

Fig. 22 to explain the deformation along explosion. According to this figure and the comparison curve shown in Fig. 23, the maximum displacement of this structure is

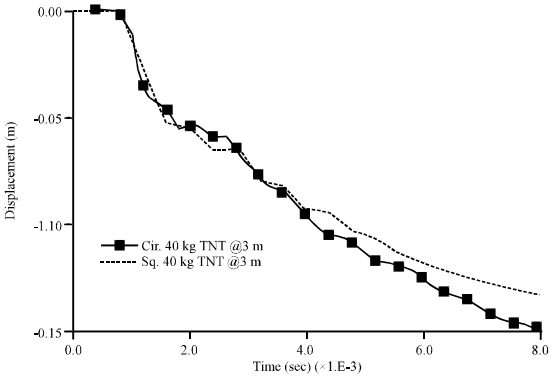

Fig. 23: Displacement history of the center of circular and square structure under explosion of 40 kg TNT

estimated to be 15.6 cm. It has to be noted that the trend of in-plate changes in this structure is almost the same as that of the square sample (Fig. 23). The legend "Sq" and "Cir" in Fig. 23 refer to square honeycomb structure and circular honeycomb structure, respectively.

Diagonal honeycomb structure was also analyzed under underwater explosion and experienced a 177 MPa stress. This stress occurred in the middle layer (core) of the honeycomb structure and its value was almost the same as the stress created in the circular structure and 27% greater than the stress in square structure. However, the behavior of the middle node in the surface plate must be considered. Given lack of allocation of boundary conditions in the software in this layer, the peripheral areas were shown to have the maximum displacement. But this model is more resistant than other samples and less displacement was experienced in the middle node. This displacement was equal to 6.9 cm which was 50% less than the displacement of other two models. The in-plate contours of the honeycomb sandwich structures with diagonal core are shown in Fig. 24 and 25. These figures elaborate the strain in upper and lower surface of the structure and show the minimum and maximum strain. According to Fig. 25, the maximum strain, occurred in the lower surface and in the vicinity of the main diameter was = 0.01 which is significantly less than that in the square sample.

In this study, the dynamic response of hexagonal honeycomb structure under explosion of 40 kg TNT is analyzed. Similar to circular structure, the hexagonal honeycomb structure experienced the maximum stress due to underwater explosion at 0.0028 sec. This stress is significantly less than the stress created in diagonal and

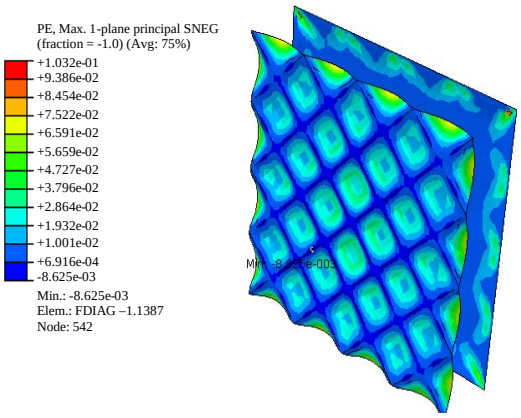

Fig. 24: Strain contours in diagonal honeycomb upper surface under explosion of 40 kg TNT

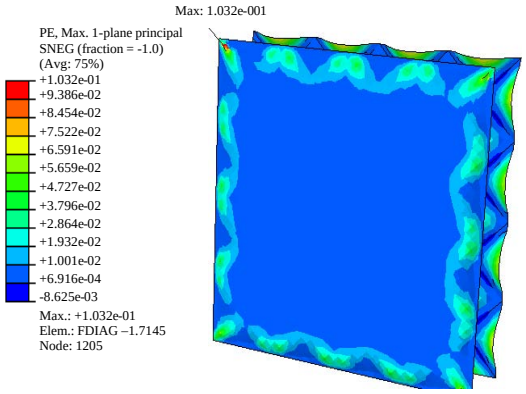

Fig. 25: Strain contours in diagonal honeycomb lower surface under explosion of 40 kg TNT

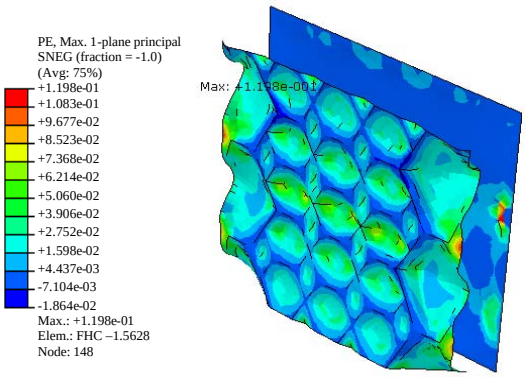

Fig. 26: Strain contours at the hexagonal upper surfaceunder explosion of 40 kg TNT

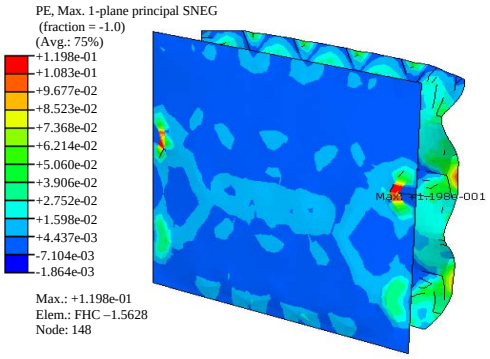

Fig. 27: Strain contours at the hexagonal lower surface under explosion of 40 kg TNT

circular samples but still greater than that in the square sample. It was determined to be 160 MPa by the software. It can also be inferred that having 12.48 cm displacement, the behavior of this structure is similar to that of the circular and square structures and still has the least displacement. Another point to be noted is ultimate strain changes in the structure. According to Fig. 26 and 27, the maximum strain at the peripheral areas facing the upper surface is 0.085 while the lower surface in the areas approaching large hexagonal sources experienced the maximum strain of 0.19. This value is close to the ultimate strain of the steel (Fig. 27) and is significant.

Applying 40 kg discharge on the discrete honeycomb structure, the 170 MPa stress as the maximum Mises stress occurred at 0.004 sec while the core layer stress at the same time was 140 MPa. The pressure resulted from underwater explosion lead to more than 19 cm displacement in the upper surface. It is clear that the displacement in the upper surface of this sample in greater than that in other samples. The ultimate strain changes are also shown in in Fig. 28 and 29. It is seen than the maximum strain occurred at peripheral areas facing the upper surface is = 0.026 while the lower surface experienced the maximum strain of 0.15 at areas approaching the larger sources of the surrounding hexagonal. According to Fig. 29, it occurred at the peripheral sides of the lower surface which is significant. According to the displacement of the middle node in the upper surface of the sandwich structure, shown in Fig. 30, the discrete honeycomb structure had the maximum deformation and displacement, = 19 cm. Other samples including square, circular, diagonal and hexagonal had 41, 20, 14 and 23% less deformation, respectively. In other words, the diagonal structure was more resistant against the waves caused by underwater explosion.

The effect of underwater explosion on kinetic and strain energy of the structure: The point to be noted in this study is that the square and discrete sample have experienced the minimum and maximum kinetic

energy, = 502 and 621 kJ, respectively. Given the different geometry of the square and discrete core it can be argued

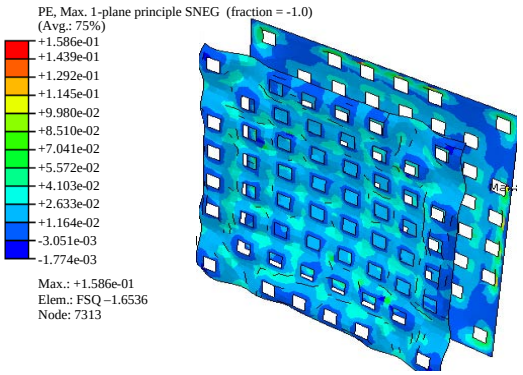

Fig. 28: Strain contours at the discrete upper surface under explosion of 40 kg TNT

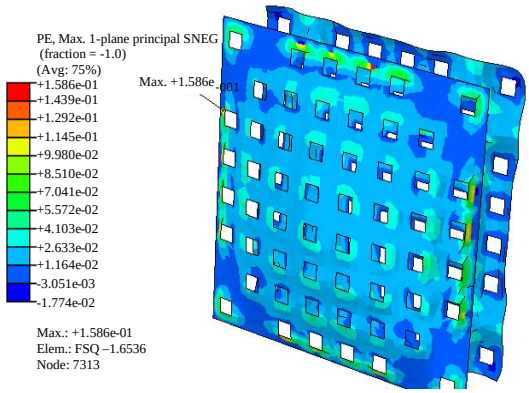

Fig. 29: Strain contours at the discrete honeycomb lower surface under explosion of 40 kg TNT

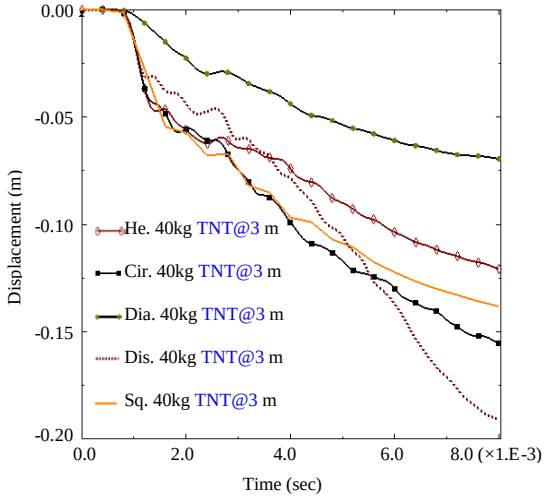

Fig. 30: Displacement history of the upper surface of all numerical models under explosion of 40 kg TNT

that due to concentration and adjacency of its core layers, the discrete honeycomb structure absorbs more kinetic energy than the square honeycomb structure with distributed core layer. This is very important when the dominant design method is based in energy absorption. The maximum energy in circular, diagonal and hexagonal samples is 562, 587 and 561 kJ, respectively which had similar maximum energy with similar changes. Figure 31 shows the changes in strain energy in 0-0.008 sec time interval due to underwater explosion.

Figure 32 shows the plot of strain energy of the structure versus time when the 40 kg TNT charge is located 3 m from the structure. It is clear that the square honeycomb structure and the discrete honeycomb structure had the maximum and minimum changes, respectively. Another point to be noted is similar behavior of diagonal and square samples and their equal under the curve area. When the design basis in the minimum strain it seems that implementing square honeycomb structure is more cost effective. The second most cost effective structure to be implemented in this case in circular honeycomb structure (Fig. 32).

Investigating the effect of increasing explosive charge on structure behavior: The explosion scenario might be not pre-determined and occur completely randomly, therefore, this study discusses charge distance in different scenarios. These scenarios are investigated for distances of 3, 4 and 7 m from the structure. The radius of the spherical waves caused by underwater explosion increases by increasing distance and the maximum pressure exerted in the structure decreases. Therefore, the structure is expected to have less deformation by

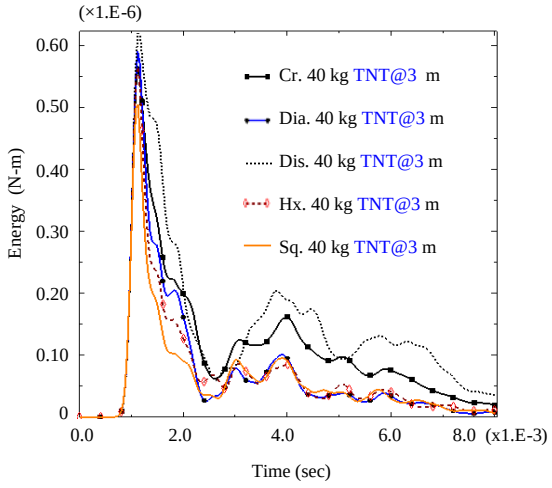

Fig. 31: History of changes in kinetic energy of the samples under explosion of 40 kg TNT

Table 8: Comparing the final displacement and kinetic energy in all samples

Parameters	Change in kinetic energy (N-M)			Middle node displacement (m)		
Charge-structure distance	7 m	4 m	3 m	7 m	4 m	3 m
Sq. honeycomb structure	74.804	272.544	505.881	-0.007	-0.030	-0.078
Cir. honeycomb structure	87.976	309.711	567.997	-0.045	-0.096	-0.156
Dia. honeycomb structure	92.430	324.640	590.932	-0.009	-0.032	-0.069
Hex. honeycomb structure	85.398	301.081	567.190	-0.027	-0.067	-0.121
Dis. honeycomb structure	105.627	340.924	620.991	-0.054	-0.127	-0.191

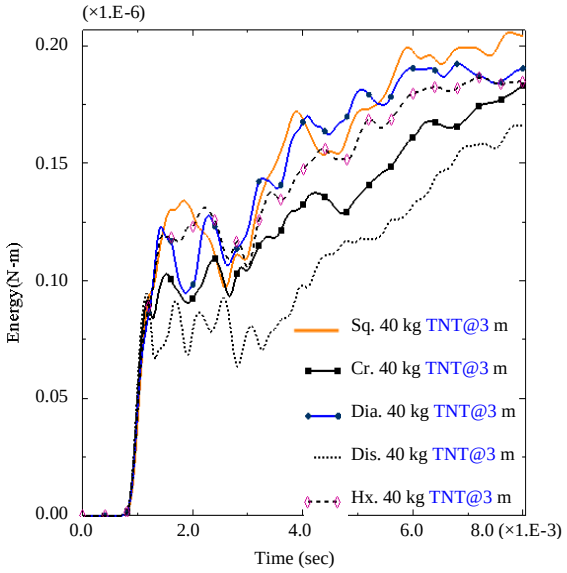

Fig. 32: History of changes in strain energy of the samples under explosion of 40 kg TNT

increasing the distance, so that, when the distance between the structure and charge in 7 m, the deformation is <1 cm. The same is true about kinetic energy of the structure and increasing distance leads to significant changes in maximum kinetic energy of the structure.

Similar to the square sample, the explosive charge was significantly changed with changing distance in the circular honeycomb structure. These changes again resulted in an inverse relationship between explosive charge distance and structure deformation, so that, the structure deformation decreased more than 3 times by increasing distance from 3-7 m. The kinetic energy of the structure also decreases by increasing the explosive charge distance. For example, the kinetic energy of square and circular structures decreases more than 6 times by increasing the distance from 3-7 m. Similar trend was observed in the diagonal sample by increasing distance for a fixed charge of 40 kg TNT. The maximum displacement of a component for 7, 4 and 3 m distance was about 1, 3 and 7 cm, respectively. Hexagonal and discrete honeycomb structures also experienced same changed in displacement and kinetic energy by increasing the distance. According to Table 8, it can be argued that charge distance has an inverse relationship with the maximum structure response which is clearly seen in all samples. Moreover, the discrete sample had the maximum structure response in all states of charge distance. On the other hand, the diagonal sample had the minimum responses in terms of displacement and energy absorbance.

CONCLUSION

The concept of structure design and reinforcement against explosion has been increasingly attended by the researchers in recent years. Therefore, the first step in this regard is simulation and analysis of the behavior of these structures during explosion. This study investigated structure design and reinforcement against underwater explosion and examined this phenomenon, analyzed the effect of charge amount in deformation of honeycomb structures as well as the effect of explosive charge distance, via. ABAQUS and numerical results were obtained. An experimental model along underwater explosion was also used for validation and reasonable results were obtained. Generally, ductility in honeycomb structures is an issue that depends on the structure core. This was frequently shown in this study in the plots, deformations, ad contours under explosion so that the discrete honeycomb structure had the maximum ductility and displacement = 19 cm. other samples including square, circular, diagonal and hexagonal had 41, 20, 14 and 23% less deformation, respectively. In other words, the diagonal structure was more resistant against the waves caused by underwater explosion.

Regarding the kinetic energy of the structure, it can be argued that the amount of this energy reaches a fairly uniform rotation in all cases after a considerable ups and downs which nearly approaches zero due to taking into account friction in modeling. It has to be noted that the discrete honeycomb structure has the maximum kinetic energy of 620 kNm which decreases by 19, 9, 9 and 5% in square, circular, hexagonal and diagonal structures, respectively. Regarding strain energy it can also be argued that the square and discrete honeycomb structures have the maximum and minimum changes in strain energy, respectively. It seem that implementing

square honeycomb structure is more cost effective and economical where the design criteria is based in minimum strain energy. Regarding the effect of the relationship between charge distance and the maximum structure response it can be inferred that these two parameters have an inverse relationship which is obvious in all simulation samples. Furthermore, the discrete sample has the maximum structure response in all cases of charge distance, so that, its in-plate displacement and kinetic energy was determined to be 20 cm and 620 kNm, respectively. On the other hand, the diagonal sample has the minimum responses in terms of displacement and energy absorbance. This ample has 6.9 cm in-plate displacement and 590 kNm kinetic energy.

ACKNOWLEDGEMENT

This Manuscript supported financially and scientifically by Iranian Port and Maritime Organization.

REFERENCES

Anonymous, 1989. Shock tests, high impact shipboard machinery, equipment and systems, Requirements. Naval Publications and Forms Center, Philadelphia.

Aruk, F., 2008. Finite element analysis of response of a floating structure to an underwater explosion. MSc Thesis, Istanbul Technical University, Saryyer, Turkey.

Cole, R.H., 1948. Underwater Explosions. Princeton University Press, Princeton, New Jersey, USA., Pages: 437.

Gupta, N.K., P. Kumar and S. Hegde, 2010. On deformation and tearing of stiffened and un-stiffened square plates subjected to underwater explosion a numerical study. Intl. J. Mech. Sci., 52: 733-744.

Hung, C.F., B.J. Lin, J.J. Hwang-Fuu and P.Y. Hsu, 2009. Dynamic response of cylindrical shell structures subjected to underwater explosion. Ocean Eng., 36: 564-577.

Klenow, B. and A. Brown, 2007. Far-Field underwater explosion (UNDEX) fluid modeling using acoustic elements. Master Thesis, Virginia Tech University, Blacksburg, Virginia.

Krueger, S.R., 2006. Simulation of cylinder implosion initiated by an underwater explosion. Ph.D Thesis, Naval Postgraduate School, Monterey, California.

Mazaheri, K. and P. Taheri, 2003. Dynamic simulation of the bubble resulted from underwater explosion using third order Lagrangian method. Military College of Engineering, Risalpur, Pakistan.

Rajendran, R. and K. Narasimhan, 2006. Deformation and fracture behaviour of plate specimens subjected to underwater explosion-a review. Int. J. Impact Eng., 32: 1945-1963.

Ramajeyathilagam, K. and C.P. Vendhan, 2004. Deformation and rupture of thin rectangular plates subjected to underwater shock. Intl. J. Impact Eng., 30: 699-719.

Shane, M.G.J., V.S. Deshpande and N.A. Fleck, 2007. The underwater blast resistance of metallic sandwich beams with prismatic lattice cores. J. Appl. Mech., 74: 352-364.

Sheng, Z.X., R.Z. Liu and R. Guo, 2012. Reverberation generated by sequential underwater explosions. Acoust. Phys., 58: 236-242.

Sprague, M.A. and T.L. Geers, 1999. Response of empty and fluid-filled, submerged spherical shells to plane and spherical, step-exponential acoustic waves. Shock Vib., 6: 147-157.

Zhang, A.M., X.L. Yao and L.H. Feng, 2009. The dynamic behavior of a gas bubble near a wall. Ocean Eng., 36: 295-305.

Zhang, P. and T.L. Geers, 1993. Excitation of a fluid-filled, submerged spherical shell by a transient acoustic wave. J. Acoustical Soc. Am., 93: 696-705.